

TOPOLOGY

Topological origin of equatorial waves

Pierre Delplace,^{1*} J. B. Marston,^{2*} Antoine Venaille^{1*}

Topology sheds new light on the emergence of unidirectional edge waves in a variety of physical systems, from condensed matter to artificial lattices. Waves observed in geophysical flows are also robust to perturbations, which suggests a role for topology. We show a topological origin for two well-known equatorially trapped waves, the Kelvin and Yanai modes, owing to the breaking of time-reversal symmetry by Earth's rotation. The nontrivial structure of the bulk Poincaré wave modes encoded through the first Chern number of value 2 guarantees the existence of these waves. This invariant demonstrates that ocean and atmospheric waves share fundamental properties with topological insulators and that topology plays an unexpected role in Earth's climate system.

Symmetries and topology are central to an understanding of physics. In condensed matter, topology explains the precise quantization of the Hall effect (1), where a magnetic field breaks the discrete symmetry of time reversal. Interest in topological properties was reinvigorated after the discovery of the quantum spin Hall effect and the subsequent classification of different states of matter according to discrete symmetries (2). Recently, topologically protected edge excitations have been found in artificial lattices of various types (3–5). A correspondence between topological properties of waves in the bulk and the existence of

unidirectional edge modes along boundaries exists in all these systems (6, 7). The edge modes fill frequency or energy gaps found in the bulk and are immune to various types of disorder. We show here that topologically protected edge waves also manifest in atmospheres and oceans.

Equatorial Kelvin and mixed Rossby-gravity (Yanai) waves are edge modes that propagate energy along Earth's equator with eastward group velocity (8). Remarkably, the dispersion relations for these waves (Fig. 1A) were derived within the framework of the rotating-shallow-water model (9) just before their first observation in the 1960s. Since then, observations of the atmosphere have

revealed a robust signature of these trapped modes in wave number–frequency spectra (10) (Fig. 1B). Equatorial Kelvin and Yanai waves have been shown to play a crucial role in several aspects of climate dynamics. For instance, Kelvin waves are a key component of the El Niño–Southern Oscillation, traveling across the waters of the Pacific Ocean (11). The waves are also part of the quasi-biennial oscillation in the stratosphere and are thought to be an important component of the Madden-Julian Oscillation in the troposphere (12).

The fact that Yanai and Kelvin waves are equatorially trapped unidirectional modes filling a frequency gap between the low-frequency planetary (Rossby) and high-frequency inertia-gravity (Poincaré) wave bands (8), as shown in Fig. 1A, suggests that they can be interpreted as topological boundary states, similar to those emerging in various topological insulating media. More precisely, bulk (Poincaré and/or Rossby) waves possess a topological property that should be directly related to the existence of these two unidirectional boundary waves by virtue of the bulk-boundary correspondence (6, 7). According

¹Université de Lyon, ENS (École Normale Supérieure) de Lyon, Université Claude Bernard, CNRS, Laboratoire de Physique, AF-69342 Lyon, France. ²Department of Physics, Box 1843, Brown University, Providence, RI 02912-1843, USA.

*Corresponding author. Email: pierre.delplace@ens-lyon.fr (P.D.); marston@brown.edu (J.B.M.); antoine.venaille@ens-lyon.fr (A.V.)

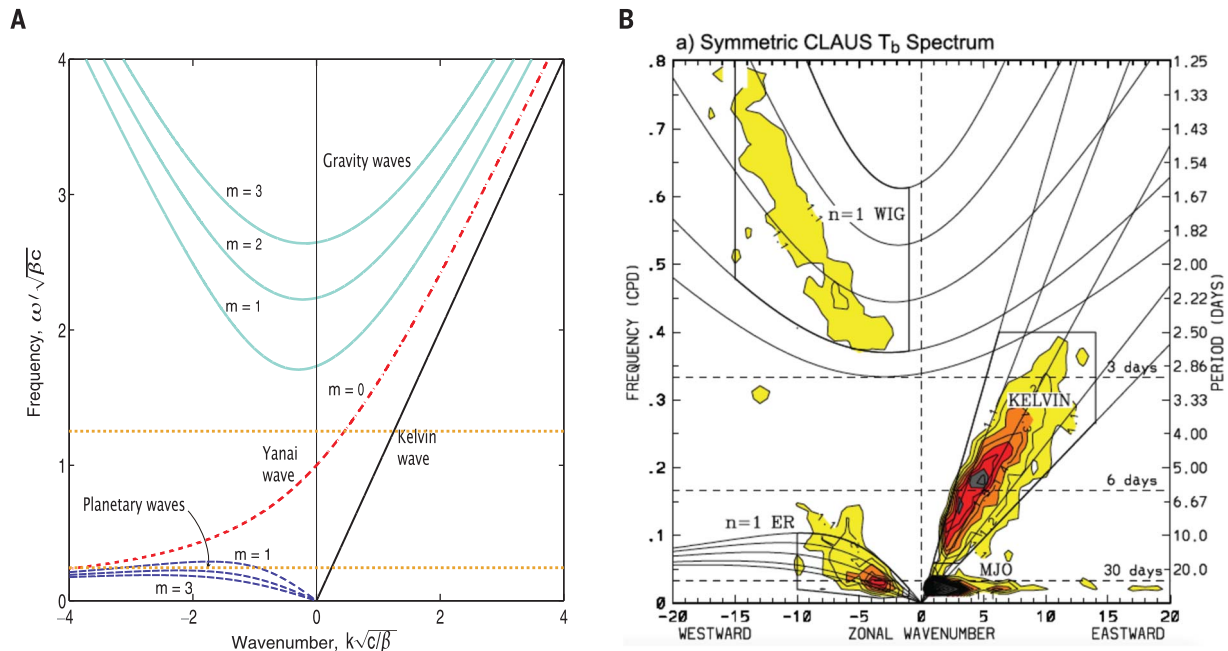


Fig. 1. Dispersion spectrum of equatorial waves. (A) Dispersion relation for shallow-water waves on an equatorial β -plane with linear variations of the Coriolis parameter with the latitude ($f = \beta y$). The dispersion relation for negative frequencies is obtained by symmetry with respect to the origin ($k = 0$, $\omega = 0$). The frequency gap between low-frequency planetary (Rossby) waves and high-frequency inertia-gravity (Poincaré) waves is filled by two modes with eastward group velocity: the equatorial Kelvin and mixed Rossby-gravity (Yanai) waves. Horizontal dotted orange lines indicate the frequencies of the

low- and intermediate-frequency wave packets used in the scattering simulation of (15). m , meridional index. [Adapted from (8)] (B) Observational evidence for the appearance of the Kelvin mode in frequency–wave number spectra of the atmosphere. Colors enclosed by contours indicate the power spectrum of the equatorially symmetric component of the CLAUUS (Cloud Archive User Services) brightness temperature T_b . WIG, westward inertia-gravity wave; ER, equatorial Rossby wave; MJO, Madden-Julian Oscillation; CPD, cycles per day. [Reproduced from (10)]

to this correspondence, the number of states inherited by a band when the zonal (directed along the equator) wave number k_x varies from $-\infty$ to $+\infty$ is given by an integer-valued topological number called the first Chern number. The first Chern number quantifies the number of phase singularities in a bundle of eigenmodes parameterized on a closed manifold. These singularities are somewhat analogous to amphidromic points ($\pm 2\pi$ phase vortices of tidal modes), but they occur in parameter space rather than in physical space. We demonstrate the existence of a non-trivial global structure in the bulk Poincaré modes as being encoded through the first Chern number of value ± 2 , thus ensuring the existence of two unidirectional edge modes at the equator that fill the two frequency gaps, in agreement with the existence of Kelvin and Yanai waves. The existence of the frequency gap originates from a broken time-reversal symmetry of the flow model owing to Earth's rotation. The structure of tidal modes (13) and bifurcations in large-scale geophysical flow (14) have previously invoked the effect of breaking time-reversal symmetry. Our study shows that another far-reaching consequence of this broken symmetry is to confer non-trivial topological properties to bundles of fluid waves, giving rise to robust edge states.

The rotating-shallow-water equations (8) that describe the dynamics of a thin layer of fluid on a two-dimensional surface of height $h(\mathbf{x}, t)$ and horizontal velocity $\mathbf{u}(\mathbf{x}, t)$ (where \mathbf{x} is the horizontal coordinate and t is time) furnish a minimal model for equatorial waves

$$\partial_t h + \nabla \cdot (h\mathbf{u}) = 0 \quad (1)$$

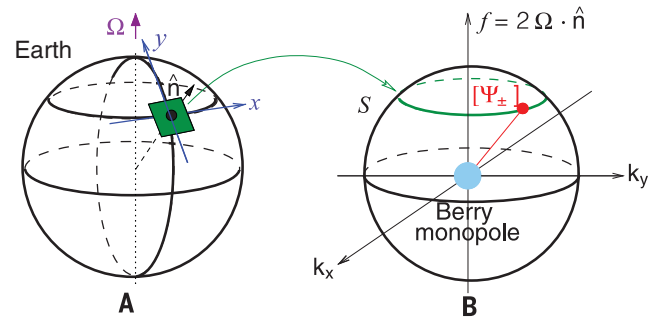
$$\partial_t \mathbf{u} + (\mathbf{u} \cdot \nabla) \mathbf{u} = -g \nabla h - f \hat{\mathbf{n}} \times \mathbf{u} \quad (2)$$

The Coriolis parameter $f = 2\boldsymbol{\Omega} \cdot \hat{\mathbf{n}}$ is twice the projection of the planetary angular rotation vector $\boldsymbol{\Omega}$ on the local vertical unit vector $\hat{\mathbf{n}}$, and g is the constant of gravitational acceleration. When linearized about a state of rest ($\mathbf{u} = 0$) and mean height ($h = H$), this dynamical system may be rewritten as $i\partial_t \Psi = \mathcal{H}\Psi$, where $\Psi = (\mathbf{u}, \eta)$ is a triplet of fields describing the two components of the perturbed velocity field and the perturbed height field η , and where \mathcal{H} is a Hermitian operator (15). Because the fields (\mathbf{u}, η) are real, the operator \mathcal{H} is equal to the negative of its complex conjugate, $\Xi \mathcal{H} \Xi^{-1} = -\mathcal{H}$, where Ξ is the operator that effects complex conjugation, with $\Xi^2 = 1$. In the quantum context, the operation is referred to as a particle-hole transformation because it inverts the spectrum. Time-reversal symmetry $t \rightarrow -t$, $\mathbf{x} \rightarrow \mathbf{x}$, $\eta \rightarrow \eta$, $\mathbf{u} \rightarrow -\mathbf{u}$ is broken by a nonzero Coriolis parameter $f \neq 0$ in Eq. 2. The broken symmetry generates gaps in the shallow-water spectrum (8).

The f -plane approximation commonly used in geophysics (8) amounts to the neglect of Earth's sphericity by assuming that the dynamics take place on a tangent plane with constant f (Fig. 2A). Translational symmetry ensures that eigenmodes of the linearized dynamics in this geometry are of the form $\Psi e^{i\omega t - ik_x x - ik_y y}$, where Ψ has three components. Viewing f/c as an external parameter,

Fig. 2. Geometry of the planetary sphere and parameter space.

(A) Relation between the spherical geometry of a rotating planet and the unbounded f -plane geometry. At a given latitude, the flow is assumed to take place in the tangent plane, and the Coriolis parameter f is twice the vertical component of



Earth's rotation. (B) Parameter space (k_x, k_y, f) for the eigenmodes on the unbounded f -plane geometry. The wave bands ω_+ , ω_- , ω_0 are well defined everywhere except at the origin, which is a band-crossing point. We show that the set of eigenmodes Ψ_+ parameterized on any closed surface (here a sphere) enclosing this band-crossing point possesses singularities that are quantified by a Chern number. This is an integer that can be computed by integrating over this surface a local Berry curvature that depends on the eigenmodes. The curvature can be viewed as generated by a Berry monopole located at the band-crossing point.

where $c = \sqrt{gH}$ is the speed of gravity waves in nonrotating shallow water, the eigenmodes may be easily found at each point in the space $(k_x, k_y, f/c)$ (Fig. 2B). There are three bands with frequencies $\omega_{\pm} = \pm(f^2 + c^2 k^2)^{1/2}$ and $\omega_0 = 0$, where $k^2 \equiv k_x^2 + k_y^2$, with corresponding wave functions $\{\Psi_+, \Psi_0\}$. For $f \neq 0$, the bands are separated by gaps of frequency f (Fig. 3). The zero-frequency modes are in geostrophic balance; the other two modes are Poincaré waves with dispersions ω_{\pm} that are symmetric with respect to the origin in (k_x, k_y, ω) space.

Eigenmodes depend on the triplet of parameters $(k_x, k_y, f/c)$ that correspond to the set of waves in all possible f -plane configurations. The eigenmodes do not vary with the distance from the origin in $(k_x, k_y, f/c)$ space and can therefore be parameterized on the surface of a sphere S that encloses the singular band-crossing point at the origin $(k_x, k_y, f/c) = (0, 0, 0)$ [Fig. 2B and (15)]. Each of the eigenstates $\{\Psi_-, \Psi_0, \Psi_+\}$ defines a fiber bundle over S that may possess topological defects. The singularities reflect the impossibility of continuously defining the eigenmodes everywhere on the sphere, particularly over both of Earth's two hemispheres simultaneously. They are quantified by the first Chern number ΔC that can be calculated for each bulk mode n as the flux of the Berry curvature $B_n = -i\nabla_p \times (\Psi_n^\dagger \nabla_p \Psi_n)$ through the sphere S , where Ψ_n^\dagger is the conjugate transpose of Ψ_n and $\nabla_p = (\partial_{k_x}, \partial_{k_y}, \partial_{f/c})$. In other words, there exists a quantized Berry flux generated by a (Berry) monopole located at the center of S , where the three bands cross (16, 17). The singularities are analogous to the one exhibited by an electron wave function that cannot be defined continuously around a Dirac magnetic monopole (18). We find $\{\Delta C_-, \Delta C_0, \Delta C_+\} = \{-2, 0, 2\}$ (15); that is, only the Poincaré modes Ψ_{\pm} are topologically non-trivial because the geostrophic modes Ψ_0 have zero Chern index, in agreement with the bulk-boundary correspondence (6, 7).

To understand qualitatively the correspondence between these bulk properties and the

emergence of unidirectional edge states in the presence of an equator, is it worth considering the case of a planar flow in an unbounded domain with f varying in the y direction from -2Ω to 2Ω (Fig. 3). Far from the interface, the eigenmodes are given by delocalized solutions—i.e., by those computed in the case of constant f . If one could continuously deform the whole set of positive-frequency eigenmodes from one hemisphere to other—for instance, by varying f slowly with y —then the eigenmodes would be given by solutions close to those calculated for constant f . Our previous calculation shows that this continuous deformation is prohibited by the occurrence of $\Delta C_{\pm} = 2$ phase singularities (positive vortices) when the plane $f = 0$ is crossed. To remove these two singularities, the positive- and negative-frequency bands must be connected to each other because the sum of their Chern numbers is zero. This connection happens through the emergence of two edge states that fill the frequency gaps. For any frequency that lies within the bulk gaps, the number of topological edge states is fixed by the set of Chern numbers (6). Because $\Delta C_{\pm} = \pm 2$, there are two extra unidirectional edge modes in the frequency gaps (15).

It is instructive to examine the Berry curvature for the Poincaré modes. As shown in Fig. 3, the curvature is mainly concentrated around $k = 0$, where it reaches extremal values, and, importantly, changes sign with f . It follows that its flux for each Poincaré mode $C_{\pm} = \frac{1}{2\pi} \int_{\text{hemisphere}} dk_x dk_y B_{\pm} = \pm \text{sgn}(f)$ is an integer that only depends on the hemisphere. It is thus tempting to say that the Poincaré eigenmodes on the two hemispheres are topologically distinct by interpreting C_{\pm} as a Chern number as well, given that the difference $C_{\pm}(f > 0) - C_{\pm}(f < 0) = \pm 2$ coincides with the first Chern number ΔC_{\pm} . This would be rigorously true if the two-dimensional manifold through which this Berry flux is computed at fixed f were closed—for instance, when the wave numbers (k_x, k_y) live on a Brillouin zone that reflects an underlying lattice. For continuous fluids, only ΔC_{\pm} is a well-defined topological

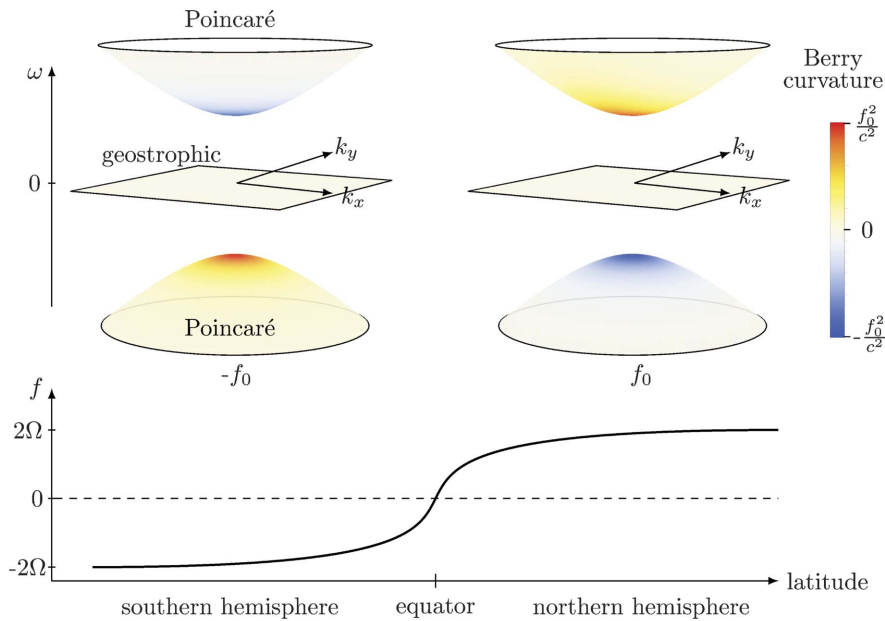


Fig. 3. Dispersion relation in unbounded f -plane geometry for the two signs of f . The color indicates the Berry curvature $B_n \equiv -i\nabla_p \times (\Psi_n^\dagger \nabla_p \Psi_n)$ for each wave band indexed by $n \in \{-, 0, +\}$. The Berry curvature of the Poincaré bands is $B_{\pm} = \pm f c^2 [f^2 + c^2(k_x^2 + k_y^2)]^{-3/2}$. It is concentrated around $k = 0$, with extremal value $\pm c^2/f^2$, and switches sign with f . The curvature vanishes for the geostrophic band. When integrated over the whole plane (k_x, k_y) , the Berry fluxes in the three bands give integers $(-1, 0, 1)$ for $f > 0$ and $(1, 0, -1)$ for $f < 0$, consistent with the triplet of Chern numbers $\{\Delta C_-, \Delta C_0, \Delta C_+\} = \{-2, 0, 2\}$. This shows that the set of delocalized bulk Poincaré modes cannot be continuously deformed from one hemisphere to another.

number, but this suffices to characterize the topological property of the bulk modes and, thus, the existence of the two equatorial unidirectional modes.

We stress one important point concerning the role of the spherical geometry of the planet in our approach. We remove this sphericity with the f -plane approximation, equivalent to holding the Coriolis parameter constant in space. However, through the construction of the sphere \mathcal{S} in parameter space $(k_x, k_y, f/c)$, we recover the effect of a varying Coriolis parameter f on the shallow-water eigenmodes. In this way, sphericity works its way back into the problem. The detailed geometry of Earth is no longer needed because topology itself requires the existence of Yanai and Kelvin waves. Even a misshapen sphere would support the waves.

Topology guarantees the existence of equatorial Yanai and Kelvin waves, obviating the need to carry out the classic but more complex calculation for the equatorial β -plane (8). On the equatorial β -plane, Rossby and Poincaré waves can also be equatorially trapped. However, this trapping depends on the precise longitudinal variation of $f(y)$, as may be demonstrated numerically. In contrast, the topological origin of Kelvin and Yanai modes makes them insensitive to the details of the interface, such as the detailed shape of $f(y)$ (15). We also performed a numerical scattering experiment showing that there is no possibility for Kelvin or Yanai waves

excited within the bulk frequency gap, away from the other bands, to exchange energy with other modes that propagate energy westward (15). Consequently, there is no energy backscattering in the presence of topography (movies S1 and S2). This robustness against disorder can now be understood as a consequence of topology.

Other ideas from topology have been applied to hydrodynamics (19–21). However, the appearance of singularities in the set of eigenmodes that arises from the breaking of time-reversal symmetry has so far been overlooked in this context, as has the physical consequence of unidirectional edge modes filling the frequency gaps. The general principle of bulk-boundary correspondence may now be applied to other fluid systems of interest.

The shallow-water system exhibits particle-hole symmetry stemming from real-valued velocity and displacement fields. More generally, any linearized fluid flow model that can be written in terms of a Hermitian operator that breaks time-reversal symmetry belongs to the symmetry class with Cartan label D, which means that nontrivial topological properties may arise (22, 23). Other physical systems that may belong to class D are chiral p -wave superconductors (16, 24) and superfluid $^3\text{He-A}$ (25). The linear operator of flow dynamics can be non-Hermitian in the presence of mean flows and dissipation, in which case other topological properties may appear (26). We expect that topology may ultimately shape

the global structure of a number of astrophysical and geophysical wave spectra where similar gaps opened in the presence of symmetry-breaking fields are known to exist. For instance, Lamb waves are edge states that fill the gap between acoustic and gravity waves because gravity breaks another discrete symmetry, that of inversion. Hall magnetohydrodynamics is another possible setting for topological edge waves (27). It will also be interesting to study in more detail the resilience of topological waves against dissipation and nonlinear wave-wave scattering processes.

REFERENCES AND NOTES

1. D. J. Thouless, M. Kohmoto, M. P. Nightingale, M. Denny, *Phys. Rev. Lett.* **49**, 405–408 (1982).
2. M. Z. Hasan, C. L. Kane, *Rev. Mod. Phys.* **82**, 3045–3067 (2010).
3. N. Goldman, J. Budich, P. Zoller, *Nat. Phys.* **12**, 639–645 (2016).
4. L. Lu, J. D. Joannopoulos, M. Soljačić, *Nat. Photonics* **8**, 821–829 (2014).
5. S. D. Huber, *Nat. Phys.* **12**, 621–623 (2016).
6. Y. Hatsugai, *Phys. Rev. Lett.* **71**, 3697–3700 (1993).
7. T. Fukui, K. Shiozaki, T. Fujiwara, S. Fujimoto, *J. Phys. Soc. Jpn.* **81**, 114602 (2012).
8. G. K. Vallis, *Atmospheric and Oceanic Fluid Dynamics: Fundamentals and Large-Scale Circulation* (Cambridge Univ. Press, ed. 2, 2017).
9. T. Matsuno, *J. Meteorol. Soc. Jpn. Ser. II* **44**, 25 (1966).
10. G. N. Kiladis, M. C. Wheeler, P. T. Haertel, K. H. Straub, P. E. Roundy, *Rev. Geophys.* **47**, RG2003 (2009).
11. L. Miller, R. E. Cheney, B. C. Douglas, *Science* **239**, 52–54 (1988).
12. C. Zhang, *Rev. Geophys.* **43**, 2004RG000158 (2005).
13. M. V. Berry, *Proc. R. Soc. London A Math. Phys. Eng. Sci.* **413**, 183–198 (1987).
14. B. Gallet, J. Herault, C. Laroche, F. Pétrélis, S. Fauve, *Geophys. Astrophys. Fluid Dyn.* **106**, 468–492 (2012).
15. See the supplementary materials.
16. B. A. Bernevig, T. L. Hughes, *Topological Insulators and Topological Superconductors* (Princeton Univ. Press, 2013).
17. M. V. Berry, *Proc. R. Soc. London A Math. Phys. Eng. Sci.* **392**, 45–57 (1984).
18. P. A. M. Dirac, *Proc. R. Soc. London A Math. Phys. Eng. Sci.* **133**, 60–72 (1931).
19. V. I. Arnold, B. A. Khesin, *Topological Methods in Hydrodynamics*, vol. 125 (Springer Science & Business Media, 1999).
20. H. K. Moffatt, in *Les Houches Session LXXIV*, M. Lesieur, A. M. Yaglom, F. David, Eds. (Springer, 2001), pp. 319–340.
21. D. Kleckner, W. T. M. Irvine, *Nat. Phys.* **9**, 253–258 (2013).
22. A. Kitaev, *AIP Conf. Proc.* **1134**, 22 (2009).
23. S. Ryu, A. P. Schnyder, A. Furusaki, A. W. Ludwig, *New J. Phys.* **12**, 065010 (2010).
24. C. Kallin, *Rep. Prog. Phys.* **75**, 042501 (2012).
25. H. Ikegami, Y. Tsutsumi, K. Kono, *Science* **341**, 59–62 (2013).
26. J. M. Zeuner et al., *Phys. Rev. Lett.* **115**, 040402 (2015).
27. E. A. Witalis, *IEEE Trans. Plasma Sci.* **14**, 842–848 (1986).

ACKNOWLEDGMENTS

We thank D. Carpentier, B. Fox-Kemper, T. Louvet, L. Maas, J. Sauls, and S. Tobias for discussions. P.D. was supported by the French Agence Nationale de la Recherche (ANR) under grant TopoDyn (ANR-14-ACHN-0031). Additional movies can be viewed at <https://vimeo.com/channels/1209812>.

SUPPLEMENTARY MATERIALS

www.sciencemag.org/content/358/6366/1075/suppl/DC1
Supplementary Text
Figs. S1 to S4
References (28–33)
Movies S1 and S2

1 June 2017; accepted 26 September 2017
Published online 5 October 2017
10.1126/science.aan8819

Topological origin of equatorial waves

Pierre Delplace, J. B. Marston and Antoine Venaille

Science **358** (6366), 1075-1077.

DOI: 10.1126/science.aan8819 originally published online October 5, 2017

Fluid waves with topological origins

Topological effects that arise from material boundaries are well known in solid-state physics and form the basis for topological insulators. Delplace *et al.* describe atmospheric and ocean waves that appear to have a similar topological origin (see the Perspective by Biello and Dimofte). The waves exist because of the symmetry-breaking nature of Earth's rotation, which allows certain fixed topological constraints on the system. These findings may be useful for understanding a wide variety of geophysical and astrophysical flows.

Science, this issue p. 1075; see also p. 990

ARTICLE TOOLS

<http://science.sciencemag.org/content/358/6366/1075>

SUPPLEMENTARY MATERIALS

<http://science.sciencemag.org/content/suppl/2017/10/04/science.aan8819.DC1>

RELATED CONTENT

[file:/content](#)

REFERENCES

This article cites 25 articles, 5 of which you can access for free
<http://science.sciencemag.org/content/358/6366/1075#BIBL>

PERMISSIONS

<http://www.sciencemag.org/help/reprints-and-permissions>

Use of this article is subject to the [Terms of Service](#)